**[Frontiers in Bioscience 7, d1212-1222, May 1, 2002]**

# INITIATION AND TERMINATION OF CALCIUM SPARKS IN SKELETAL MUSCLE

**Martin F. Schneider and Christopher W. Ward**

*Department of Biochemistry and Molecular Biology, University of Maryland School of Medicine, 108 N. Greene St, Baltimore, MD 21201*

## TABLE OF CONTENTS

*1. Abstract*
*2. General background and early observations of $Ca^{2+}$ sparks*
- *2.1. Excitation-contraction coupling*
- *2.2. "Macroscopic" and "Microscopic" SR $Ca^{2+}$ release in muscle fibers*
- *2.3. Initial observations of $Ca^{2+}$ sparks in skeletal muscle*
- *2.4. Considerations in imaging $Ca^{2+}$ sparks*
  - *2.4.1. Generation of a $Ca^{2+}$ spark*
  - *2.4.2. Out of focus events: effects on rise-time and amplitude*
  - *2.4.3. Rep-mode events exhibit constancy of released $Ca^{2+}$*
  - *2.4.4. Number of channels in the confocal volume at a triad*

*3. Voltage-activated $ca^{2+}$ sparks*
- *3.1. Repriming protocol for studying voltage-activated events*
- *3.2. Initiation of $Ca^{2+}$ sparks during step depolarization*
- *3.3. Pattern of occurrence of $Ca^{2+}$ sparks determines release wave form*
- *3.4. RyR isoforms and voltage sensor coupling to RyRs*

*4. Time course of $Ca^{2+}$ release during an individual spark*
- *4.1. Abrupt turn-on and turn-off of $Ca^{2+}$ release in a spark*
- *4.2. Voltage sensor restoration can prematurely terminate $Ca^{2+}$ release in voltage-activated sparks*
- *4.3. $Ca^{2+}$ release channel activity underlying a spark*

*5. Ligand activated $Ca^{2+}$ sparks*
- *5.1. Permeablized fibers for the manipulation of cytosolic ligands*
- *5.2. Activation of $Ca^{2+}$ sparks by physiological ligands*

*6. Modulation of $Ca^{2+}$ sparks by exogenous peptides in permeabilized fibers*
- *6.1. Prolonged $Ca^{2+}$ channel opening by Imperatoxin A: long duration $Ca^{2+}$ sparks*
- *6.2. RyR domain peptide DP4 increases $Ca^{2+}$ spark frequency but does not alter spark properties*
- *6.3. Multimeric Homer protein induces $Ca^{2+}$ sparks in frog skeletal muscle but does not alter spark properties*

*7. Conclusions*
*8. Acknowledgements*
*9. References*

## 1. ABSTRACT

Depolarization of the transverse tubules of a skeletal muscle fiber initiates release of $Ca^{2+}$ ions via ryanodine receptor (RyR) $Ca^{2+}$ release channels in the adjacent junctional sarcoplasmic reticulum (SR) membrane at triad junctions. Discrete localized $Ca^{2+}$ release events ($Ca^{2+}$ "sparks") detected by confocal imaging of $Ca^{2+}$ indicator-containing muscle fibers may arise from the coordinated opening of a small group of RyR $Ca^{2+}$ release channels, or possibly even from the opening of a single channel. These discrete $Ca^{2+}$ release events originate at triad junctions and can be gated by fiber depolarization or by physiological cytosolic ligands (e.g., $Ca^{2+}$ and $Mg^{2+}$) in functioning muscle fibers. The global increase in myoplasmic $Ca^{2+}$ during fiber depolarization appears to consist of the summation of huge numbers of $Ca^{2+}$ sparks initiated during a brief time interval. Study of $Ca^{2+}$ sparks thus offers a unique window into the operation of groups of SR $Ca^{2+}$ release channels or individual channels within the normal structural and molecular environment of a functioning fiber. The $Ca^{2+}$ release underlying a spark appears to turn on and off abruptly respectively at the start and at the peak of a spark. Under many stimuli, the frequency and/or pattern of occurrence of the $Ca^{2+}$ sparks is altered, indicating changes in the closed time (or opening rate) of the channels that initiate the sparks. In contrast, the average values of the spatio-temporal properties of the individual events generally remain unchanged, indicating constancy of channel open time and constancy of total $Ca^{2+}$ efflux via the channels generating a spark. A few conditions that alter the average properties of $Ca^{2+}$ sparks provide rare insights regarding the open-time of the $Ca^{2+}$ channels generating the $Ca^{2+}$ spark.

## 2. GENERAL BACKGROUND AND EARLY OBSERVATIONS OF $Ca^{2+}$ SPARKS

### 2.1. Excitation-contraction coupling

Activation of skeletal muscle occurs over a time scale of msec or at most a few tens of msec. Special systems have evolved for achieving relatively large and fast release of calcium ions from the calcium-sequestering internal membrane system (SR) in skeletal muscle. Ryanodine receptor (RyR) $Ca^{2+}$ release channels in the SR terminal cisternae membrane have a large cytosolic domain, the junctional foot, that spans the gap between the junctional SR and the adjacent transverse tubule (TT) and thus provides a structural basis for rapid direct or indirect molecular interaction between an RYR and a dihydropyridine receptor (DHPR) voltage sensor in the TT membrane. The voltage sensor responds to the change in TT membrane potential and directly initiates physiological $Ca^{2+}$ release from the apposed RyR $Ca^{2+}$ release channel without the need for entry of $Ca^{2+}$ ions form the extracellular solution, the hallmark of "skeletal-type" EC coupling.

### 2.2. "Macroscopic" and "Microscopic" SR $Ca^{2+}$ release in muscle fibers

Average cytosolic [$Ca^{2+}$] transients due to the combined activity of large numbers of calcium release channels in a single muscle fiber have been monitored by many laboratories in functionally intact skeletal muscle fibers. Such global or "macroscopic" $Ca^{2+}$ transients have been analyzed to calculate the time course of the overall rate of release of calcium from the SR in our own (1, 2) and other (3) laboratories. The resulting release wave form, which exhibits an early peak followed by a decline to a more maintained steady level during a voltage clamp depolarization (1), corresponds to the "macroscopic" calcium efflux through the population of SR calcium release channels throughout the muscle fiber, equivalent to a macroscopic calcium current across the SR membrane. In 1995 "microscopic" calcium release events ($Ca^{2+}$ "sparks"), which may underlie the macroscopic calcium release waveform, were detected in skeletal muscle (4, 5) after having been first identified in cardiac myocytes (6). The $Ca^{2+}$ sparks presumably occur in such high frequency and large numbers during depolarization of a muscle fiber that the individual events become indistinguishable during the macroscopic [$Ca^{2+}$] transient (7). The development of experimental conditions under which $Ca^{2+}$ sparks could be observed and characterized constituted a major advance in the study of SR $Ca^{2+}$ release in skeletal muscle. The ability to monitor $Ca^{2+}$ sparks has revolutionized the study of SR channel behavior in functioning muscle fibers (e.g., 8, 9, 10). Because of their robust properties and ease of experimental manipulation, single, cut or permeabilized frog twitch skeletal muscle fibers have been utilized for the studies reviewed here unless otherwise indicated.

### 2.3. Initial observations of $Ca^{2+}$ sparks in skeletal muscle

Our early work on $Ca^{2+}$ sparks, as well as work at the same time in the Rios laboratory, developed procedures for studying both voltage activated and "spontaneous" (i.e., ligand-activated) $Ca^{2+}$ sparks in skeletal muscle fibers. By using an extracellular dye that enters the transverse tubules and thus marks their location (11), we were able to identify the TT location in our fibers and to establish that voltage activated $Ca^{2+}$ sparks were centered at the triads (7), as were the spontaneous release events. This is as expected since the calcium release channels are localized in the junctional SR membrane at the triad.

Our initial results showed that calcium sparks occurred during small depolarizations of fully polarized frog cut skeletal muscle fibers voltage clamped in a double Vaseline gap chamber and also occurred "spontaneously" in fully polarized or fully depolarized fibers (5, 7). As in cardiac myocytes (6), these events were thought to correspond to the opening of functionally linked groups of a few SR calcium release channels or even of individual SR channels.

In fully polarized fibers, discrete $Ca^{2+}$ sparks could be resolved only during relatively small depolarizations because during larger depolarizations the individual events were obscured by the large overall rise in fluorescence. However, over the limited range of depolarizations during which discrete events could be discerned, the event frequency increased steeply with increasing depolarization (e-fold in about 3 to 4 mV; (7)). We thus hypothesize that the macroscopic calcium transient generated during full activation of a fiber is due to the combined result of large numbers of discrete release events occurring at a frequency that is too high to allow resolution of individual events. The ability to detect and characterize these discrete release events provides an exciting and novel approach to gaining new understanding of SR channel activity in functioning muscle fibers.

### 2.4. Considerations in imaging $Ca^{2+}$ sparks

#### 2.4.1. Generation of a $Ca^{2+}$ spark

Following the initiation of a $Ca^{2+}$ spark there is a rise in local fluorescence (Figure 1) that is comprised of an increase in the concentration of $Ca^{2+}$-fluo-3 within the confocal volume. This implies that $Ca^{2+}$ entry into the confocal volume must exceed the net effect of $Ca^{2+}$ "removal" by binding and diffusion out of the confocal volume. Thus, during the rising phase of a spark, $Ca^{2+}$ ions are being released from the channel or channels responsible for generating the spark. In contrast, during the falling phase of fluorescence in a spark, there is a net reduction of $Ca^{2+}$-fluo-3 in the confocal volume, indicating that $Ca^{2+}$ binding and $Ca^{2+}$ diffusion out of the confocal volume exceed $Ca^{2+}$ entry. Since the diffusion and $Ca^{2+}$ binding properties of the myofibril are unlikely to change significantly during the spark, the declining phase of a spark must correspond to a period during which $Ca^{2+}$ release occurs at a much lower rate than during the rising phase. In the extreme case, following spark activation $Ca^{2+}$ release could occur at an approximately constant rate during the rising phase of the spark, and then stop completely during the falling phase. The duration of the rising phase of a $Ca^{2+}$ spark thus provides a lower bound estimation of the time of $Ca^{2+}$ release from the channel or channels generating the spark. Furthermore, the time course of the rising phase of a spark may provide important information concerning the degree of synchrony of possible multiple channels generating the spark. In contrast, the

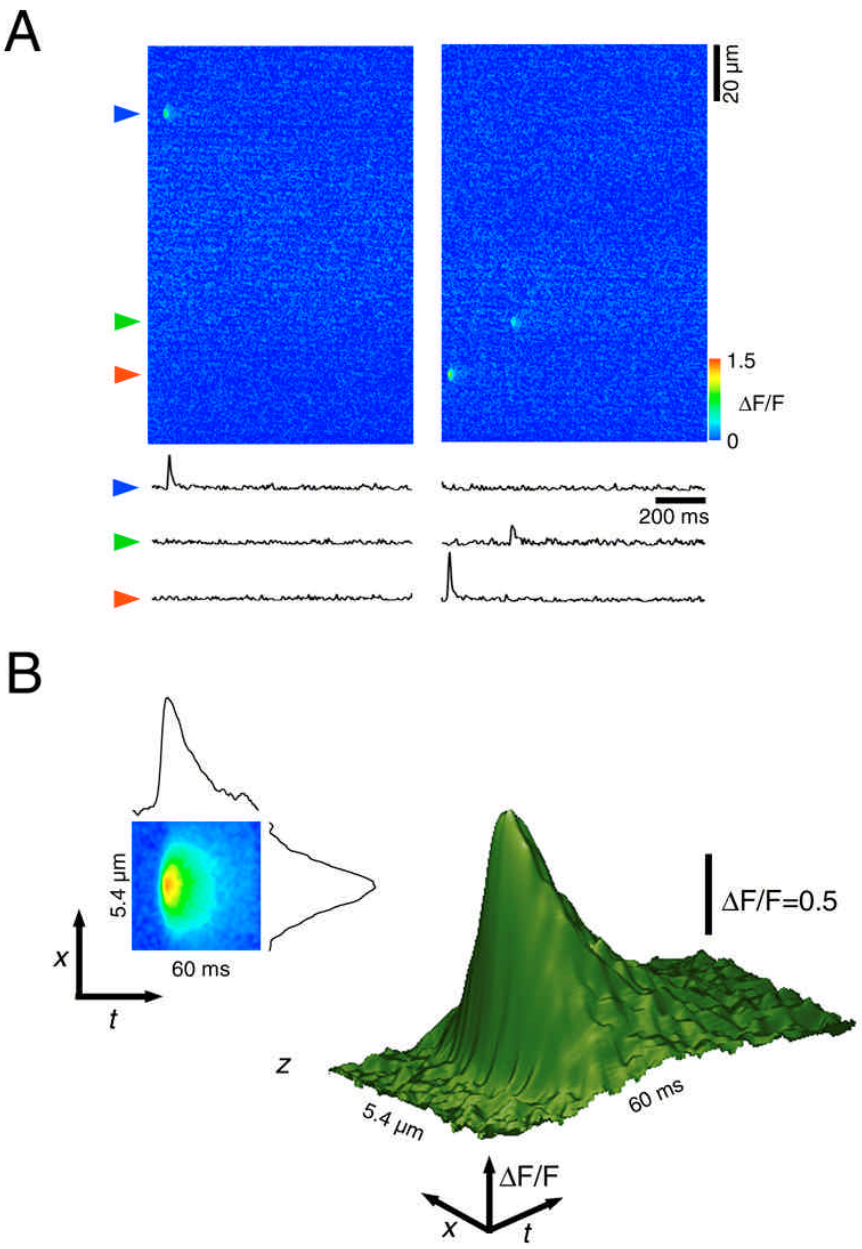


**Figure 1.** $Ca^{2+}$ sparks in frog skeletal muscle. **A.** Two successive line scan images (2 ms/line, 1 sec total time/image, pseudo-color ΔF/F presentation) of a permeablized frog skeletal muscle fiber equilibrated with Fluo-3 containing internal solution ($[Mg^{2+}]_{free}$=0.65) are presented. Three $Ca^{2+}$ sparks are apparent as discrete localized increases in fluorescence. Temporal ΔF/F fluorescence profiles of select spatial locations (arrowheads) are presented below. **B.** 93 $Ca^{2+}$ sparks were spatially centered and temporally shifted to the 50% rise-time to construct a signal averaged event. The pseudo-color *xt* plot (left) is presented with spatial and temporal fluorescence profiles extracted through the peak of the fluorescence. A surface plot representation (right) provides a view of the temporal and spatial characteristics of the averaged $Ca^{2+}$ spark. The mean values (±) SEM of the spatio-temporal properties of the sparks averaged to give the mean event were 10-90% rise time 5.6 ± 0.2 ms, full duration at half max (FDHM) 11.9 ± 0.3 ms, full width at half max (FWHM) 1.6 ± 0.1 µm and peak amplitude (ΔF/F) 1.2 ± 0.1.

spark amplitude, which depends on both duration and magnitude of the rate of $Ca^{2+}$ efflux via the channels generating the spark, provides an indication of the total amount of $Ca^{2+}$ released in the event.

#### 2.4.2. Out of focus events: effects on rise-time and amplitude

One technique used to image spatially localized, subcellular fluorescent transients (e.g., $Ca^{2+}$ sparks) is the use of a laser scanning confocal microscope (LSCM) in conjunction with $Ca^{2+}$ indicator dyes. The LSCM limits the spatial sampling of fluorescence based on its ability to physically limit the detection of emission photons which are out of the focus volume of the microscope objective. This spatially restricted sampling volume can be estimated by examining the point spread function of the LSCM, which for our consideration, can be roughly approximated as a spherical volume of approximately 1µm diameter. While confocal imaging provides restricted spatial sampling ability, the interpretation of the fluorescence signal (i.e., the shape of the $Ca^{2+}$ spark) can be affected by $Ca^{2+}$ diffusing out of the plane of focus as well as by events occurring some distance from the scanned line. Numerical simulation of the $Ca^{2+}$ spark morphology as a function of the distance of $Ca^{2+}$ spark generation from the sampling volume results in significant decrease in amplitude of the spark with increasing distance from the sampled volume, but much less alteration in the rise-time (12, 13)

#### 2.4.3. Rep-mode events exhibit constancy of released $Ca^{2+}$

Under conditions of very low activation, voltage activated and ligand activated $Ca^{2+}$ sparks appear in a stochastic manner and on average occur very rarely at any given triad. As an exception to this, a second mode of $Ca^{2+}$ spark activation (*rep*-mode) was identified in which, at low levels of overall activation, $Ca^{2+}$ release events occurred repetitively in a single triad at rates >100 fold the rate in the remaining triads (14). The events within a given *rep*-mode train were of similar amplitude and spatio-temporal extent, suggesting that each of these events arose from release of the same amount of $Ca^{2+}$ from a given group of channels within the same triad. Analysis of the inter-spark intervals revealed a lack of repetitive events occurring at very short intervals. The mean recovery time (98 ms) was similar to the time constant for recovery of the underlying $Ca^{2+}$ release channel(s) from $Ca^{2+}$ dependent inactivation (50 - 100 ms; 15, 16) prior to subsequent reactivation in the train. Additionally, the population of sparks within the *rep*-mode trains were similar in spatio-temporal characteristics to a population of singly occurring sparks in the same fibers consistent with a common mode of inactivation for both groups. Since the events in a rep-mode train arise from the same $Ca^{2+}$ release unit in a given triad, all are the same distance from the scan line and thus are all recorded with the same relative distortion of amplitude and rise-time.

#### 2.4.4. Number of channels in the confocal volume at a triad

It is important to take into account the structural composition of the skeletal muscle triad when interpreting the confocal imaging of $Ca^{2+}$ release. A detailed consideration of the shape, size and distribution of calcium release units and the functional coupling of these units to voltage sensors (i.e., couplons) has recently been published (17) Due to the limited scope of this review, we limit our consideration to an estimate of the number of $Ca^{2+}$ release channels sampled at each triad during confocal line scan imaging. In frog twitch fibers, a 1µm diameter sphere, which very roughly approximates the sampled confocal volume, includes about 50-100 RyR $Ca^{2+}$ release channels at each triad.

## 3. VOLTAGE-ACTIVATED $Ca^{2+}$ SPARKS

### 3.1. Repriming protocol for studying voltage-activated events

In fully polarized fibers, voltage elicited $Ca^{2+}$ sparks can only be clearly discerned during small depolarizations, which severely limits the study of voltage dependence of these events. In order to study voltage activated $Ca^{2+}$ sparks over the entire range of membrane potentials, we exploited a "repriming" protocol (18, 19) to avoid the large [$Ca^{2+}$] transients that would otherwise obscure any discrete events during large depolarizations of fully polarized fibers. Starting with a chronically depolarized muscle fiber, we restore only a small fraction of the TT DHPR voltage sensors from the inactivated ("immobilized") state by brief repolarization (20, 21) and then activate the restored voltage sensors by depolarization (Figure 2). We found that when a small group of reprimed voltage sensors is driven to their activating conformation by a large depolarization after brief repriming, calcium sparks similar to those activated by small depolarization of the same fully polarized fiber were observed (19). $Ca^{2+}$ released from RyRs coupled to and directly opened by activated voltage sensors may secondarily activate neighboring RyRs (Figure 2) by calcium induced calcium release (CICR). Although it is impossible to resolve individual events during large depolarizations in a fully primed fiber, our results to date with partially reprimed fibers appear to be consistent with the hypothesis that large macroscopic releases are composed of the summation of a large number of individual calcium sparks occurring at a high frequency. Thus, knowledge of the properties of the underlying release events provides crucial information for understanding of the macroscopic voltage activated calcium release in a fully primed Fiber.

### 3.2. Initiation of $Ca^{2+}$ sparks during step depolarization

Following brief repriming of a chronically depolarized fiber, step depolarizations reveal discrete $Ca^{2+}$ sparks occurring at individual triads. Analysis of the frequency of event occurrence relative to the start of a depolarization (i.e., latency histogram) provides an indication of the voltage dependent gating pattern of the available $Ca^{2+}$ channels at the triad. Our results show that during a large depolarization, which should rapidly and maximally activate all reprimed voltage sensors, the event latency histogram exhibits a marked early peak, corresponding to a burst of sparks within the first few ms of the pulse, followed by a much lower maintained steady rate of sparks (10). By using a moderate repriming time, the full voltage dependence of the frequency of events both during the peak rate at the start of a pulse, and during the steady level later in the pulse was determined (10). With increasing voltage, an increase in the total event frequency as well as an increase in the clustering of events near the initiation time of the voltage pulse was evident. In addition, analysis determined no differences in

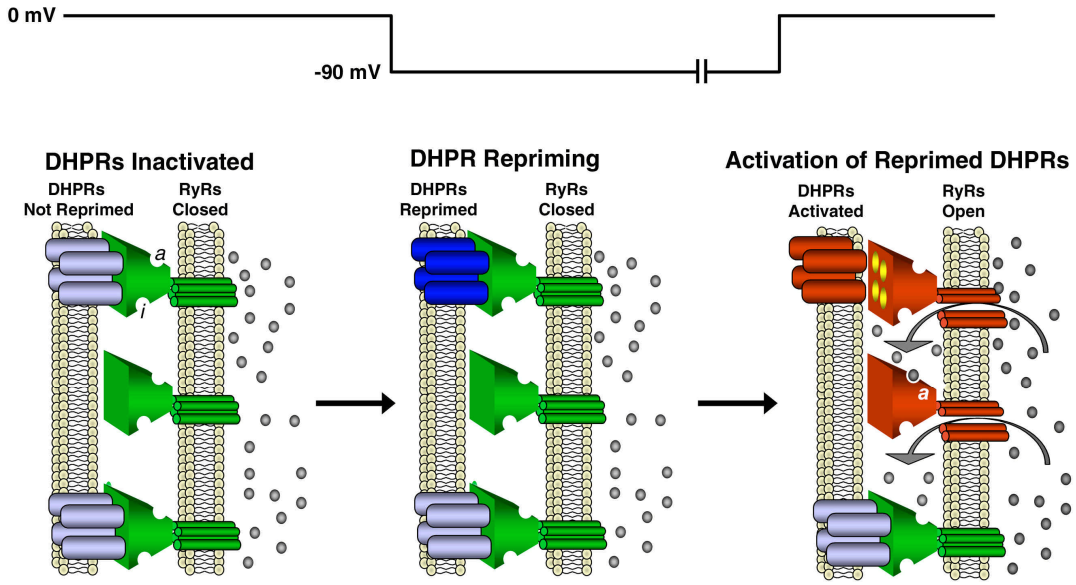


**Figure 2.** Cartoon depiction of the proposed states of the DHPR and RyR following brief repriming and subsequent depolarization in a chronically depolarized frog skeletal muscle fiber. DHPR voltage sensors are depicted as coupling with alternating RyRs (22 ). Ligand ($Ca^{2+}$/$Mg^{2+}$) binding sites for activation by $Ca^{2+}$ (*a*) and inactivation (*i*) by $Ca^{2+}$ of $Mg^{2+}$ are represented on each RyR $Ca^{2+}$ release channel. Chronic fiber depolarization to 0 mV leads to inactivation of DHPR voltage sensors. In this condition the DHPRs coupled to RyRs are unable to initiate RyR opening. During a brief repriming period to –90 mV, a small fraction of the DHPRs are reprimed for activation (blue DHPR, top) and subsequent depolarizations activate the reprimed DHPRs (red) and initiate RyR (red) $Ca^{2+}$release from RyRs coupled to the activated DHPR voltage sensor. $Ca^{2+}$ release from the voltage coupled RyR channel can also activate neighboring RyRs to open by CICR due to the locally elevated [$Ca^{2+}$].

spatio-temporal properties of the $Ca^{2+}$ sparks based on position of occurrence relative to the pulse suggesting that the underlying channel behavior and conductance was voltage independent.

### 3.3. Pattern of occurrence of $Ca^{2+}$ sparks determines release wave form

Since the properties of $Ca^{2+}$ sparks were voltage independent, we could assume that the rate of $Ca^{2+}$ efflux via the open channel(s) underlying a spark to be on average the same for all events. We then could use the latency histogram together with the mean spark rise time (which provides a measure of the overall time for $Ca^{2+}$ efflux during each event) to construct a time course of $Ca^{2+}$ release from the SR due to the identified sparks (10). For large depolarizing test pulses we obtained a peaked release wave form, generally similar to the macroscopic rate of release wave forms calculated previously from average global [$Ca^{2+}$] transients in fully polarized fibers (1, 3), but possibly showing a somewhat more pronounced peak. Based on these findings, we were able to conclude that the voltage dependence in the $Ca^{2+}$ release flux waveform is due to the temporal occurrence of individual $Ca^{2+}$ sparks whose individual properties are independent of voltage.

### 3.4. RyR isoforms and voltage sensor coupling to RyRs

RyRs coupled to TT voltage sensors (DHPRs) alternate with non-coupled RyRs along a “checkerboard” double row in toadfish swim bladder muscle (22), and the same arrangement may occur in frog muscle. Two RyR isoforms, 1 and 3 or their homologues (alpha and beta in amphibian muscle) are expressed in skeletal muscle. RyR1 but not 3 organizes DHPRs (23, 24) and supports skeletal EC coupling (25). Thus, the coupled RyRs (Fig 1) must be RyR1. Toadfish swim bladder expresses only RyR1, so by inference the intervening non-coupled RyRs in frog muscle could also be RyR1. In that case, RyR3, which is expressed at the same level as RyR1 in frog muscle, would be located in the recently described row of non-coupled parajunctional RyR’s (26) that runs on either side of the double row of alternating coupled and non coupled RyRs (above). The functional significance for $Ca^{2+}$ sparks of such a possible isoform arrangement remains to be determined. However, in the dyspedic myotube cell system, exclusive expression of RyR3 causes the appearance of both isolated and *rep*-mode $Ca^{2+}$ sparks having properties very similar to $Ca^{2+}$ sparks in frog skeletal muscle fibers (27). Furthermore, myotubes from both RyR1 (28) and RyR3 (29, 30) KO mice exhibit $Ca^{2+}$ sparks, as do dyspedic myotubes expressing RyR1 (31) and adult mammalian muscle fibers expressing exclusively RyR1 (32). Thus either isoform seems capable of generating a $Ca^{2+}$ spark

## 4. TIME COURSE OF $Ca^{2+}$ RELEASE DURING AN INDIVIDUAL SPARK

### 4.1. Abrupt turn-on and turn-off of $Ca^{2+}$ release in a spark

Studies of $Ca^{2+}$ sparks in both skeletal and cardiac muscle have used laser scanning confocal

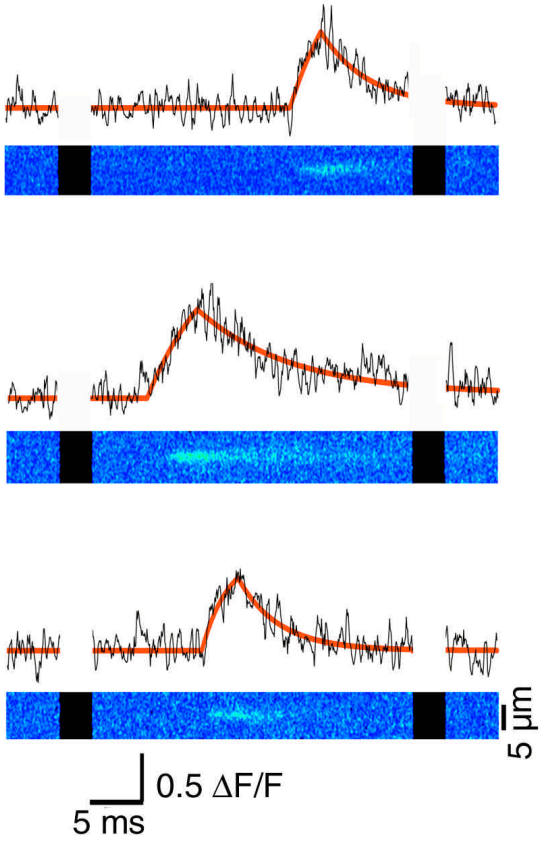


**Figure 3.** Representative $Ca^{2+}$ sparks imaged at a substantially higher time resolution (63 µs/line) than in standard imaging methods (2 ms/line). ΔF/F image strips of individual $Ca^{2+}$ sparks as well as the corresponding ΔF/F fluorescent transient monitored at the spatial center of the spark are shown. Black gaps in the image represent time gaps between successive *xt* images. The time course of each $Ca^{2+}$ spark is fit to a function that empirically reproduced the main features of the observed time courses (see text).

microscope systems with galvanometer mirrors which scan the sample at rates of 1.5-2 ms per line. Since the rising phase of a typical $Ca^{2+}$ spark is on the order of 4-6 ms, these systems provide only 2-3 time points, which is clearly insufficient to resolve details of the kinetics of the rising phase of the spark. In order to investigate the kinetic detail of $Ca^{2+}$ sparks we have used a confocal system based on a resonant galvonometer for increased speed of scanning. This system, developed by Dr. Roger Tsien (33) and subsequently developed commercially by Nikon (RCM 8000) is used to image $Ca^{2+}$ spark events at the standard video rate of 63 µs per scan line, about 30 times faster than conventional confocal systems. Figure 3 displays a representative image strip of a $Ca^{2+}$ spark as well as corresponding ΔF/F fluorescence transient monitored at the spatial center of the spark. The ΔF/F time course of each individual $Ca^{2+}$ spark imaged was characterized by fitting each record to a function that empirically reproduced the main features of these observed time courses (34). This function (i.e., sequence of 2 exponentials), which provides a discontinuous rate of change at start and peak of the spark, was able to accurately reproduce most aspects of the $Ca^{2+}$ spark time course. Results from two studies (34, 35) demonstrate a very abrupt initiation of fluorescence beginning at a maximal mono-exponential rate and continuing through the rising phase of the spark. The rising phase was followed by an abrupt transition from rising to falling fluorescence at the peak of the spark. The falling phase then followed a mono-exponential decaying timecourse. These findings are consistent with a large, rapid and relatively constant $Ca^{2+}$ release during the rising phase followed by abrupt decrease in the rate of $Ca^{2+}$ release rate at the peak of the spark.

### 4.2. Voltage sensor restoration can prematurely terminate $Ca^{2+}$ release in voltage-activated sparks

In recent studies of $Ca^{2+}$ sparks using the high speed confocal system, we have investigated the question of whether sparks which are initiated by the voltage sensors during fiber depolarization remain under voltage sensor control after their initiation. To investigate this question we examined $Ca^{2+}$ sparks produced by depolarizing test pulses which were relatively long (15-60 ms) relative to the spark rise time with $Ca^{2+}$ sparks produced by pulses which were short (3-6 ms) relative to the spark rise time. The rationale behind this comparison was that during the short pulses, the voltage sensors could deactivate at the end of the pulse during the rising phase of a spark when the $Ca^{2+}$

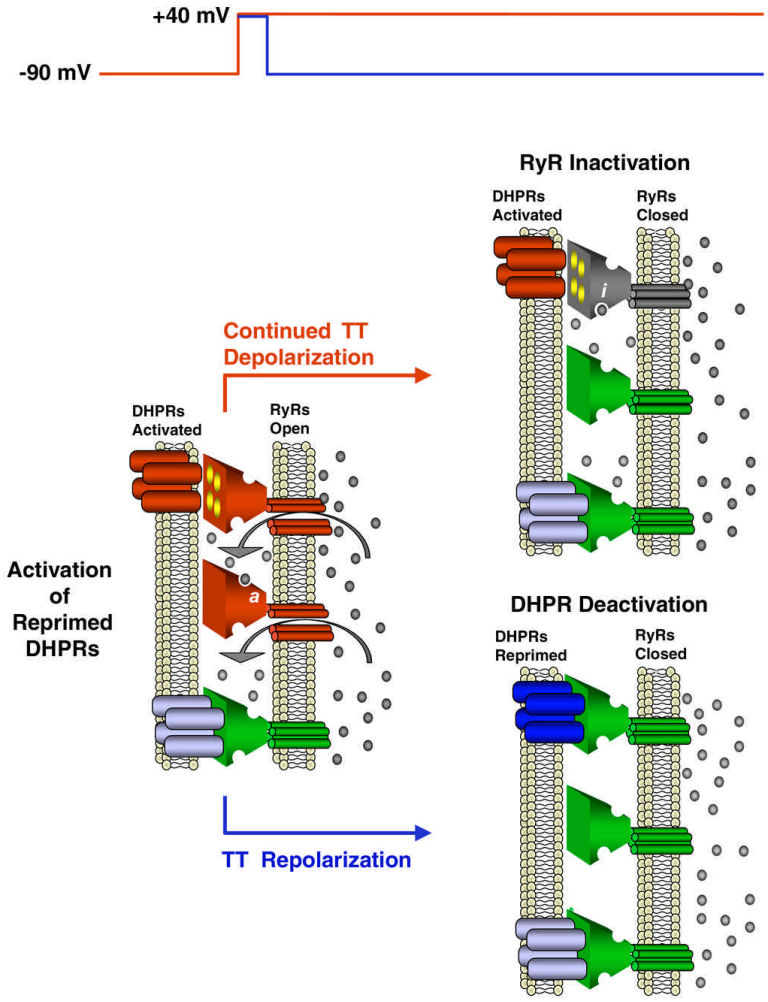


**Figure 4.** Cartoon interpretation of the two mechanisms of termination of $Ca^{2+}$ sparks. Following the activation of RyR $Ca^{2+}$ release channels by reprimed and subsequently depolarized voltage sensors (red), continued depolarization (top) results in inactivation of the RyRs (gray). Inactivation occurs most likely through ligand induced $Ca^{2+}$ inactivation mechanism at both the voltage sensor coupled RyR (occupied *i* site) and the uncoupled RyR (inactivation not shown). Alternatively, during brief depolarization (bottom) reprimed DHPRs are deactivated (blue) causing premature closing of the coupled RyR.

release in the spark was still occurring (Figure 4). If the voltage sensor were required for continued activity of the SR $Ca^{2+}$ release channels generating the spark, then the channels would be prematurely closed after the short pulse. In this case the rising phase of the spark would consequently be briefer that that of a spark during a long depolarization. Our results in fact showed that the mean duration of the rising phase (3.6 ms) of sparks elicited by 3 - 6 ms pulses was significantly shorter than the mean duration of the rising phase (4.5 ms) of sparks elicited by longer duration pulses (35). Furthermore, the spark rise time decreased systematically the later the spark initiation time occurred relative to the end of the pulse. This result indicates that deactivation of voltage sensors provides one mechanism for terminating the SR $Ca^{2+}$ release channel activity underlying a $Ca^{2+}$ spark. The distance along the TT-SR junction over which the DHPR coupled RyR exerts an influence on neighboring RyRs, and the possible role of conformational coupling of adjacent RyRs (36) in this voltage sensor control remain to be determined. During longer duration depolarizing pulses, when the voltage sensor is continuously active, the rising phase of a spark is also terminated (above). Therefore there must also be an inactivation mechanism that terminates the SR $Ca^{2+}$ release channel activity underlying a spark even during the continued activation signal from the voltage sensor. Thus, the SR $Ca^{2+}$ release channel openings underlying a spark can be terminated by either of two alternative mechanisms (Figure 2): either by voltage sensor deactivation, as occurs after short depolarizations, or by SR channel inactivation during more prolonged depolarizations. Spontaneous $Ca^{2+}$ sparks, which appear to be initiated independent of voltage sensors, are activated by ligand interaction with the RyR and would be terminated by inactivation, also independently of the voltage sensor.

### 4.3. $Ca^{2+}$ release channel activity underlying a spark

From our results presented above, it does not seem implausible that $Ca^{2+}$ release underlying a spark could be initiated at its maximal rate and then could turn off abruptly and completely at the peak of a spark. In this case the rise time of the spark would correspond to the total time that the channel or group of channels generating the spark were open, and the declining phase would be a time during which the release rate were zero. As discussed previously, (37) this interpretation could correspond to a single channel open for the entire rising phase of the spark. Alternatively, multiple channels, each of which remain open throughout the rising phase of the spark, or multiple channels that open and close asynchronously and repeatedly during the rising phase of the spark but which all close within a short interval at the time of peak of the spark would also be consistent with our observations.

Recent work by the Rios laboratory (38) has provided new data regarding channel activity underlying voltage activated $Ca^{2+}$ sparks. Under conditions in which the CICR potential was low (high $[Mg^{2+}]$ in the internal solution), voltage elicited $Ca^{2+}$ sparks were spatially narrowed and exhibited a low amplitude, prolongation (ember; <100ms) of fluorescence. In the presence of caffeine (high CICR potential), voltage elicited $Ca^{2+}$ sparks were spatially more extensive than in the control condition and did not present with ember fluorescence. Additionally, under control conditions there was some indication of the presence of the ember. These authors postulate that the low CICR potential reduced the recruitment of channels contributing to the $Ca^{2+}$ spark, thereby revealing an 'ember' fluorescence. This sustained low amplitude fluorescence was attributed to a single channel which is controlled by voltage sensor activation and remains open at low CICR potential despite the suppression of $Ca^{2+}$ release by RyRs activated secondarily via CICR. In this case the channel closing scheme for long depolarizations in Figure 4 would have to be modified to show RyRs activated by CICR closing before the voltage activated channel at low CICR potential, but not at high CICR potential. In this model it is postulated that a "master" channel, activated by the TT voltage sensor, synchronizes the opening of neighboring $Ca^{2+}$ release channels during voltage activated $Ca^{2+}$ sparks at high, but not at low CICR potential. However, in this case the mechanism by which CICR activation terminates the voltage activated ember remains to be determined.

In the most general interpretation, the rise time of a spark provides a lower limit for the open time of channels responsible for generating the spark. Some channel(s) might open or remain open during the declining phase, even though the rate of release must have been markedly less than during the rising phase (preceding paragraph). These types of interpretation can be made quantitative through the use of detailed modeling of $Ca^{2+}$ binding and diffusion in a fiber after $Ca^{2+}$ release from a channel or group of channels. (e.g., 12, 13). Unfortunately detailed discussion of these models is beyond the scope of this brief review; however, these quantitative models (12, 13) indicate that release could abruptly turn on and off at the start and peak of the observed sparks.

## 5. LIGAND ACTIVATED $Ca^{2+}$ SPARKS

### 5.1. Permeablized fibers for the manipulation of cytosolic ligands

Spontaneous $Ca^{2+}$ sparks have been visualized in fully polarized as well as in chronically depolarized fiber preparations (5, 7). These events are thought to be initiated by ligand activation, most likely through calcium-induced-calcium-release (CICR) mechanisms. Several techniques have been used to investigate ligand activated $Ca^{2+}$ sparks in depolarized fiber preparations, the purpose of all such techniques being to introduce $Ca^{2+}$ indicator dye and possible modulators (e.g., ions, small peptides) into the cytosol. Techniques such as mechanical disruption (e.g., notched, peeled fiber preparations) or chemical permeablization (e.g., saponin, ionophore) are effective tools for this approach in skeletal and cardiac cells. In recent investigations we have used brief saponin permeablization, which provides a rapid equilibration of experimental solutions, including large molecules (i.e., peptides ($IPTx_a$) and small proteins (Homer)), into and out of skeletal fibers (39). The permeablized fibers exhibit spontaneous $Ca^{2+}$ sparks which have properties quantitatively similar to spontaneous $Ca^{2+}$ sparks imaged in mechanically notched fibers (40) as well as voltage activated sparks.

### 5.2. Activation of $Ca^{2+}$ sparks by physiological ligands

Cytosolic $Ca^{2+}$ and $Mg^{2+}$ ions are known physiologic modulators of SR $Ca^{2+}$ release. Based on a model adapted from Laver et al. (41) we expect that as $[Mg^{2+}]$ is lowered, $Mg^{2+}$ first dissociates from a low affinity inactivation site ("*i*" site) at which binding of either $Ca^{2+}$ or $Mg^{2+}$ inhibits channel opening. $Mg^{2+}$ then dissociates from the high affinity $Ca^{2+}$ activation site ("*a*" site") at which either $Ca^{2+}$ or $Mg^{2+}$ can bind, but at which only $Ca^{2+}$ activates the channel. Thus, $Mg^{2+}$ binding at this site competitively inhibits $Ca^{2+}$ activation of the channel. After $Mg^{2+}$ dissociates from the site, $Ca^{2+}$ can bind to the ion-free site in a subsequent step in which the channel actually opens via a CICR dependent mechanism.

We have examined the effect of myoplasmic free $[Mg^{2+}]$ on the frequency and properties of spontaneous $Ca^{2+}$ sparks. Initial studies were carried out using "notched" (and consequently depolarized) segments challenged with various concentrations of free $[Mg^{2+}]$ and ~100nM $[Ca^{2+}]_{free}$ (38). As myoplasmic $[Mg^{2+}]$ was lowered, the frequency of $Ca^{2+}$ sparks increased, indicating a pronounced increase in the activation rate of the channel or channels responsible for initiation the $[Ca^{2+}]$ sparks. Over the $[Mg^{2+}]$ range of about 0.1 to 2 mM, the event frequency increased in inverse proportion to the 1.6 power of $[Mg^{2+}]$, consistent with at least 2 $Mg^{2+}$ ions being involved in binding at an inhibitory site for channel opening, which is consistent with the model put forward by Laver (41). In recent studies we have confirmed this $[Mg^{2+}]$ dependence using saponin permeabilized fibers, in which equilibration of cytosolic solutions is more rapid and is uniform along the length of the fiber (42).

Despite the steep rise in spark activation with decreasing cytosolic $[Mg^{2+}]$, the mean amplitude, amplitude distribution, mean rise time, rise time distribution, and the

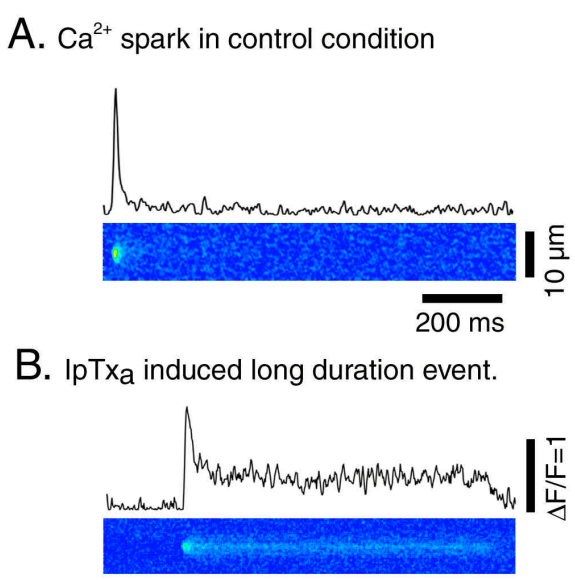


**Figure 5. A.** 1024 ms ΔF/F image strip containing a single $Ca^{2+}$ spark. The temporal fluorescent transient is presented above. The spark appears as a discrete, transient fluorescent increase within this image strip. **B.** Image strip and corresponding ΔF/F time-course of long duration $Ca^{2+}$ release event induced by application of 5 nM $IpTx_a$. The sustained low amplitude fluorescence is apparent throughout the majority of the image strip and can be present with (this figure) or without (not shown) the presence of a discrete $Ca^{2+}$ spark.

spatial spread of the sparks were all the same at each $[Mg^{2+}]$ level tested (40). These observations indicate that while the rate of $Ca^{2+}$ spark activation was dramatically affected by $[Mg^{2+}]$, the inactivation kinetics of the $Ca^{2+}$ spark was independent of $[Mg^{2+}]$. Consequently, the average open time of the channel or channels underlying a spark was also presumably independent of $[Mg^{2+}]$, since it is unlikely that the SR $Ca^{2+}$ content was changed during the experiment. Since raising $[Mg^{2+}]$ does not appear to speed the inactivation process, we conclude that the channels that opened following $Mg^{2+}$ dissociation from the inhibitory site must close by some process independent of the rebinding of $Mg^{2+}$ to the inhibitory site. Channel closing independent of $Mg^{2+}$ could be achieved by $Ca^{2+}$ binding to the inactivation site due to locally high $Ca^{2+}$ in the immediate vicinity of the open channel.

According to the above scheme, $Ca^{2+}$ is the activator of the channel in "spontaneous" (i.e., ligand activated) events, which are thus initiated by calcium–induced calcium release (CICR). Increasing the frequency of occurrence of $Ca^{2+}$ sparks can be demonstrated by increasing $[Ca^{2+}]$ in internal solutions exposed to notched (7) or permeablized fibers. However, the increased indicator fluorescence accompanying the elevated $[Ca^{2+}]$, as well as the possibility of increased SR $Ca^{2+}$ loading, make cytosolic $Ca^{2+}$ a less convienent tool for manipulating spark frequency than cytosolic $Mg^{2+}$.

## 6. MODULATION OF $Ca^{2+}$ SPARKS BY EXOGENOUS PEPTIDES IN PERMEABILIZED FIBERS

### 6.1. Prolonged $Ca^{2+}$ channel opening by Imperatoxin A: long duration $Ca^{2+}$ sparks

Imperatoxin A ($Iptx_a$) is a 33 amino acid peptide that structurally resembles the $Thr^{671}$-$Leu^{690}$ portion of the dihydropyridine receptor II-II loop. In the planar lipid bilayer, this peptide interacts with single frog RyR's and induces long-lasting substates of ~30% of full current amplitude. In saponin permeablized frog skeletal muscle fibers, 5nM $IpTx_a$ induced long duration (mean = 1.8 sec), relatively small (~ 30% of control spark peak amplitude) release events that occurred either with or without sparks superimposed on the fluorescence substate (39; Figure 5). The fluorescence waveforms were consistent with the "long openings" to subconductance state, often superimposed with full conductance openings, induced by $IpTx_a$ in lipid bilayers (43). The frequency of occurrence of long duration $IpTx_a$-induced events increased in proportion to $[IpTx_a]$ in a manner consistent with results from single channel recordings of RyRs in bilayers. The mean duration of the peptide-induced long duration events were independent of toxin concentration and agreed closely with the mean duration of subconductance states seen in the bilayer where $IpTx_a$ induced opening of single frog RyR channels to a subconductance state. These results suggest involvement of a single molecule of $IpTx_a$ in the activation of a single RyR channel to produce the long duration event. Thus binding of a single $IpTx_a$ molecule to an RyR overrides the inactivation mechanism which would normally close the channel and terminate the spark. In this respect, $IpTx_a$ is unique as the only compound we have observed to alter closing properties of the channels underlying a $Ca^{2+}$ spark.

### 6.2. RyR domain peptide DP4 increases $Ca^{2+}$ spark frequency but does not alter spark properties.

DP4 is a 36-residue synthetic peptide, which corresponds to the $Leu^{2442}$-$Pro^{2477}$ region of RyR1. Based on single channel studies, it has been proposed that DP4 disrupts the normal interdomain interactions that stabilize the closed state of the $Ca^{2+}$ release channel ((44); and review in this issue) thereby promoting $Ca^{2+}$ channel activation. We investigated the effects of DP4 on $Ca^{2+}$ sparks in saponin-permeablized frog skeletal muscle fibers (42). DP4 caused a significant concentration dependent increase in $Ca^{2+}$ spark frequency. However, the mean values of the amplitude, rise time, spatial half width and temporal half duration of the $Ca^{2+}$ sparks, as well as the distribution of these parameters, remained essentially unchanged in the presence of DP4. Thus, DP4 increased the rate of activation of the RyR $Ca^{2+}$ release channels initiating the $Ca^{2+}$ sparks but, unlike $IpTx_a$, had no effect on the inactivation kinetics. The same peptide with an $Arg^{17}$ to $Cys^{17}$ replacement (DP4mut), which corresponds to the $Arg^{2458}$-to-$Cys^{2458}$ mutation in malignant hyperthermia (MH), did not produce a significant effect on RyR activation in muscle fibers, bilayers, or SR vesicles. The lack of effect of DP4mut is consistent with the inability of this mutated peptide to form a high affinity interaction with

its complimentary domain in the RyR. Thus, DP4mut would not interfere with the intrinsic interdomain interaction within the RyR. In MH, a failure of the corresponding mutated domain to interact with the same complimentary domain would tend to destabilize the RyR conformation, thereby promoting channel opening. $Mg^{2+}$-dependence experiments conducted with permeablized muscle fibers indicate that DP4 referentially binds to partially $Mg^{2+}$-free RyR(s), thus promoting channel opening and $Ca^{2+}$ spark activation (42).

### 6.3. Multimeric Homer protein induces $Ca^{2+}$ sparks in frog skeletal muscle but does not alter spark properties

Homer protein H1c binds plasma membrane $Ca^{2+}$ channels and/or internal $Ca^{2+}$ release channels through an EVH1 domain and cross-links such membrane proteins via self-multimerization of the homer proteins at their coiled-coil (CC) domain (45). These proteins have recently been shown to bind to RyR and to increase RyR channel open probability (46). We have examined the effects of homer proteins on spontaneous $Ca^{2+}$ sparks in permeablized frog skeletal muscle fibers (47). Homer protein H1c [5-50nM], which has both EVH1 and CC domains, initiated a concentration dependent increase in spontaneous $Ca^{2+}$ spark frequency with no change in the spatial or temporal properties of the $Ca^{2+}$ sparks. Homer H1a, which has the EVH1 domain but lacks the CC domain and thus cannot cross link channels, had no effect on $Ca^{2+}$ sparks. A non-binding EVH1 mutant (mutH1c) of H1c, applied at 10 fold higher concentration than H1c, had no effect on $Ca^{2+}$ spark frequency or properties. However, when H1c was applied together with 10-fold excess mutH1c, the effect of H1c was prevented. This is consistent with mutH1c and H1c forming heteromeric dimers having one binding and one non-binding end, resulting in a dominant negative inability of H1c to cross link channels. It thus appears that the activation of $Ca^{2+}$ sparks in permeablized frog skeletal muscle fibers is potentiated by Homer proteins, but only if the cross-linking capability is present. Homer proteins, however, do not affect channel closing and total amount of $Ca^{2+}$ released since spark rise-time and amplitude are unchanged.

## 7. CONCLUSIONS

At the global level, the increase in myoplasmic $Ca^{2+}$ during fiber depolarization appears to consist of the summation of huge numbers of $Ca^{2+}$ sparks during a brief time interval. Therefore, insights into the processes by which $Ca^{2+}$ sparks are modulated could offer insight into the functioning of SR $Ca^{2+}$ release channel(s). At the local level, $Ca^{2+}$ spark activation can be initiated by either voltage or ligand dependent mechanisms. The frequency of occurrence of these events provides information concerning the rate of opening of RyR channels initiating $Ca^{2+}$ sparks, whereas the amplitude and rise-time provide indication of the amount of $Ca^{2+}$ release and the effective open time of the RyR channels generating a $Ca^{2+}$ spark.

## 8. ACKNOWLEDGEMENTS

We gratefully acknowledge the many contributions of present and former members of this laboratory, as well as our outside collaborators, Drs. H. Valdivia, P.D. Allen, N. Ikemoto and their laboratories, to our work presented here. Our work was supported by NIH grants R01-NS23346 to M.F.S, K01-AR02177 to C.W.W and the Interdisciplinary Training Program in Muscle Biology (NIH T32-AR07592), and by a research grant from the National Science Foundation (MCB-9724045 to M.F.S.)

## 9. REFERENCES

1. Melzer W, Rios E, Schneider MF: Time course of calcium release and removal in skeletal muscle fibres. *Biophys.J.* 45:637-641 (1984)
2. Melzer W, Rios E, Schneider MF: A general procedure for determining calcium release from the sarcoplasmic reticulum in skeletal muscle fibers. *Biophys.J.* 51:849-863 (1987)
3. Baylor SM, Chandler WK, Marshall MW: Sarcoplasmic reticulum calcium release in frog skeletal muscle fibres estimated from Arsenazo III calcium transients. *J Physiol* 344:625-666 (1983)
4. Tsugorka A, Rios E, Blatter LA: Imaging elementary events of calcium release in skeletal muscle cells. *Science* 269:1723-1726 (1995)
5. Klein MG, Cheng H, Santana LF, Lederer WJ, Schneider MF: Stochastic calcium release events activated by dual mechanisms at triad junctions in skeletal muscle. *J.Gen.Physiol.* 106(6):44A.(1995)
6. Cheng H, Lederer WJ, Cannell MB: Calcium sparks:elementary events underlying excitation-contraction coupling in heart muscle. *Science* 262:740-744 (1993)
7. Klein MG, Cheng H, Santana LF, Jiang Y-H, Lederer WJ, Schneider MF: Two mechanisms of quantized calcium release in skeletal muscle. *Nature* 379:455-458 (1996)
8. Shirokova N, Rios E: Small events $Ca^{2+}$ release: a probable precursor of $Ca^{2+}$ sparks in frog skeletal muscle. *J.Physiol.* 502(1):3-11 (1997)
9. Stern MD, Pizarro G, Rios E: Local control model of excitation-contraction coupling in skeletal muscle. *J Gen Physiol* 110:415-440 (1997)
10. Klein MG, Lacampagne A, Schneider MF: Voltage dependence of the pattern and frequency of discrete $Ca^{2+}$ release events after brief repriming in frog skeletal muscle. *Proc.Natl.Acad.Sci.U.S.A.* 94:11061-11066 (1997)
11. Endo M. Entry of fluorescent dyes into the sarcotubular system of the frog muscle. *J.Physiol.* 185:224-238 (1966)
12. Pratusevich VR, Balke CW: Factors shaping the confocal image of the calcium spark in cardiac muscle cells. *Biophys.J.* 71:2942-2957 (1996)
13. Jiang YH, Klein MG, Schneider MF: Numerical simulation of $Ca^{2+}$ "Sparks" in skeletal muscle. *Biophys.J.* 77:2333-2357 (1999)
14. Klein MG, Lacampagne A, Schneider MF: A repetitive mode of activation of discrete $Ca^{2+}$ release events ($Ca^{2+}$ sparks) in frog skeletal muscle fibres. *J Physiol* 515 ( Pt 2):391-411 (1999)
15. Jong D-S, Pape PC, Baylor SM, Chandler WK: Calcium inactivation of calcium release in frog cut muscle fibers that contain millimolar EGTA or fura-2. *J.Gen.Physiol.* 106:337-388 (1995)
16. Schneider MF, Simon BJ: Inactivation of calcium release from the sarcoplasmic reticulum in frog skeletal muscle. *J.Physiol.* 405:727-745 (1988)

17. Franzini-Armstrong C, Protasi F, Ramesh V: Shape, size, and distribution of Ca($^{2+}$) release units and couplons in skeletal and cardiac muscles. *Biophys J* 77:1528-1539 (1999)
18. Hodgkin AL, Horowicz P: Potassium contractures in single muscle fibres. *J.Physiol.* 153:386-403 (1960)
19. Lacampagne A, Lederer WJ, Schneider MF, Klein MG: Repriming and activation alter the frequency of stereotyped discrete $Ca^{2+}$ release events in frog skeletal muscle. *J.Physiol.(Lond.)* 497:581-588 (1996)
20. Chandler WK, Rakowski RF, Schneider MF: Effects of glycerol treatment and maintained depolarization on charge movement in skeletal muscle. *J Physiol* 254:285-316 (1976)
21. Adrian RH, Chandler WK, Rakowski RF: Charge movement and mechanical repriming in skeletal muscle. *J Physiol* 254:361-388 (1976)
22. Block BA, Franzini-Armstrong C: The structure of the membrane systems in a novel muscle cell modified for heat production. *J.Cell Biol.* 107:1099-1112 (1988)
23. Protasi, F., Franzini-Armstrong, C., Allen, P.D. Role of ryanodine receptors in the assembly of calcium release units in skeletal muscle. *J.Cell Biol.* 140:831-842 (1998)
24. Protasi F, Takekura H, Wang Y, Chen SR, Meissner G, Allen PD, Franzini-Armstrong C: RYR1 and RYR3 have different roles in the assembly of calcium release units of skeletal muscle. *Biophys J* 79:2494-2508 (2000)
25. Fessenden JD, Wang Y, Moore RA, Chen SR, Allen PD, Pessah IN: Divergent functional properties of ryanodine receptor types 1 and 3 expressed in a myogenic cell line. *Biophys J* 79:2509-2525 (2000)
26. Felder E, Franzini-Armstrong C: Type 3 ryanodine receptors of skeletal muscle are segregated in a parajunctional position *Proc Natl Acad Sci U S A* 99:1695-1700 (2002)
27. Ward CW, Schneider MF, Castillo D, Protasi F, Wang Y, Chen SR, Allen PD: Expression of ryanodine receptor RyR3 produces $Ca^{2+}$ sparks in dyspedic myotubes. *J Physiol* 525 Pt 1:91-103 (2000)
27. Shirokova N, Garcia J, Rios E: Local calcium release in mammalian skeletal muscle. *J Physiol* 512 ( Pt 2):377-384 (1998)
28. Shirokova N, Shirokov R, Rossi D, Gonzalez A, Kirsch WG, Garcia J, Sorrentino V, Rios E: Spatially segregated control of $Ca^{2+}$ release in developing skeletal muscle of mice. *J.Physiol.(Lond.)* 521 Pt 2:483-495 (1999)
29. Conklin MW, Ahern CA, Vallejo P, Sorrentino V, Takeshima H, Coronado R: Comparison of $Ca^{2+}$ sparks produced independently by two ryanodine receptor isoforms (type 1 or type 3). *Biophys J* 78:1777-1785 (2000)
30. Ward CW, Protasi F, Castillo D, Wang Y, Chen SR, Pessah IN, Allen PD, Schneider MF,: Type 1 and Type 3 ryanodine receptors generate different $Ca^{2+}$ release event activity in both intact and permeablized myotubes. *Biophys. J* 81: (2001) *in press*
31. Kirsch W.G., Uttenweiler D., Fink R.H.A., Spark- and ember-like elementary $Ca^{2+}$ release in skinned fibres of adult mammalian skeletal muscle, *J. Physiol* (2001) *in press*
32. Tsien RY, Bacskai BJ. Video-rate confocal microscopy. In: Pawley JB, ed. *Handbook of Biological Confocal Microscopy.* New York: Plenum Press, 1995:459-477.
33. Lacampagne A, Ward CW, Klein MG, Schneider MF: Time course of individual $Ca^{2+}$ sparks in frog skeletal muscle recorded at high time resolution. *J.Gen.Physiol.* 113:187-198 (1999)
34. Lacampagne A, Klein MG, Ward CW, Schneider MF: Two mechanisms for termination of individual $Ca^{2+}$ sparks in skeletal muscle. *Proc Natl Acad Sci U S A* 97:7823-7828 (2000)
35. Marx,S.O. Ondrias,K. Marks,A.R: Coupled gating between individual skeletal muscle $Ca^{2+}$ release channels (Ryanodine receptors). Science 281, 818-821. 1998.
36. Schneider MF. $Ca^{2+}$ sparks in frog skeletal muscle: generation by one, some, or many SR $Ca^{2+}$ release channels? *J.Gen.Physiol.* 113:365-372 (1999)
37. Gonzalez A, Kirsch WG, Shirokova N, Pizarro G, Stern MD, Rios E: The spark and its ember: separately gated local components of Ca($^{2+}$) release in skeletal muscle. *J.Gen.Physiol.* 115:139-158 (*2000)*
38. Shtifman A, Ward CW, Wang J, Valdivia HH, Schneider MF: Effects of imperatoxin A on local sarcoplasmic reticulum Ca($^{2+}$) release in frog skeletal muscle. *Biophys J* 79:814-827 (2000)
39. Lacampagne A, Klein MG, Schneider MF: Modulation of the frequency of spontaneous sarcoplasmic reticulum $Ca^{2+}$ release events ($Ca^{2+}$ sparks) by myoplasmic [$Mg^{2+}$] in frog skeletal muscle. *J.Gen.Physiol.* 111:207-224 (1998)
40. Laver DR, Baynes TM, Dulhunty AF: Magnesium inhibition of ryanodine receptor calcium channels: evidence for two independent mechanisms. *J.Membrane Biol.* 156:213-229 (1997)
41. Shtifman AS, Ward CW, Yamamoto T, Wang J, Olbinski B, Valdivia HH, Ikemoto N, Schneider MF: Interdomain Interactions within Ryanodine Receptors Regulate $Ca^{2+}$ Spark Frequency in Skeletal Muscle. *J Gen Physiol* (2002) *in press*
42. Tripathy A, Resch W, Xu L, Valdivia HH, Meissner G: Imperatoxin A induces subconductance states in $Ca^{2+}$ release channels (ryanodine receptors) of cardiac and skeletal muscle. *J Gen Physiol* 111:679-690 (1998)
43. Ikemoto N, Yamamoto T: Postulated role of inter-domain interaction within the ryanodine receptor in $Ca^{2+}$ channel regulation. *Trends Cardiovasc Med* 10:310-316 (2000)
44. Xiao B, Tu JC, Petralia RS, Yuan JP, Doan A, Breder CD, Ruggiero A, Lanahan AA, Wenthold RJ, Worley PF: Homer regulates the association of group 1 metabotropic glutamate receptors with multivalent complexes of homer-related, synaptic proteins. *Neuron* 21:707-716 (1998)
45. Feng, W, Tu JC, Tianzhong Y, Worley, PF, Allen PD, Pessah IN Homer regulates gain of ryanodine receptor complex *Biophys J* (82), 392a (2002)
46. Ward CW, Tu JC, Worley PF, Schneider MF Multimeric Homer protein induces $Ca^{2+}$ sparks in frog skeletal muscle *Biophys J* (82), 1374a (2002)

**Key words:** Ryanodine Receptor, Calcium Spark, Dihydropyridine Receptor, Calcium Channel, Voltage Sensor, Review

**Send correspondence to:** Martin Schneider, Ph.D., Dept. of Biochemistry and Molecular Biology, University of Maryland School of Medicine, 108 N. Greene St, Baltimore MD, 21201 Tel: 410-706-7812, Fax: 410-706-8297, E-mail: mschneid@umaryland.edu